

# Effect of Temperature Dependency on Thermoelastic Behavior of Rotating Variable Thickness FGM Cantilever Beam

M.M.H. Mirzaei, A. Loghman<sup>\*</sup>, M. Arefi

*Department of Solid Mechanics, Faculty of Mechanical Engineering, University of Kashan, Kashan, Iran*

Received 25 June 2019; accepted 27 August 2019

## ABSTRACT

Thermoelastic behavior of temperature-dependent (TD) and independent (TID) functionally graded variable thickness cantilever beam subjected to mechanical and thermal loadings is studied based on shear deformation theory using a semi-analytical method. Loading is composed of a transverse distributed force, a longitudinal distributed temperature field due to steady-state heat conduction from root to the tip surface of the beam and an inertia body force due to rotation. A successive relaxation (SR) method for solving temperature-dependent steady-state heat conduction equation is employed to obtain the accurate temperature field. The beam is made of functionally graded material (FGM) in which the mechanical and thermal properties are variable in longitudinal direction based on the volume fraction of constituent. Using first-order shear deformation theory, linear strain–displacement relations and Generalized Hooke's law, a system of second order differential equation is obtained. Using division method, differential equations are solved for every division. As a result, longitudinal displacement, transverse displacement, and consequently longitudinal stress, shear stress and effective stress are investigated. The results are presented for temperature dependent and independent properties. It has been found that the temperature dependency of the material has a significant effect on temperature distribution, displacements and stresses. This model can be used for thermoelastic analysis of simple turbine blades.

© 2019 IAU, Arak Branch. All rights reserved.

**Keywords:** Cantilever beam; Temperature dependency; Functional graded materials (FGM); First-order shear deformation theory (FSDT); Division method; Thermoelastic.

## 1 INTRODUCTION

THE variable thickness cantilever beams have great applications in many static and dynamic structures. Analysis of variable thickness cantilever beams made of isotropic material is one of the conventional problems which have been already investigated in many literatures. A group of scientists developed a novel class of materials, which

<sup>\*</sup>Corresponding author. Tel.: +98 03155913400.  
E-mail address: [aloghman@kashanu.ac.ir](mailto:aloghman@kashanu.ac.ir) (A. Loghman).

is known as functionally graded material (FGM), with desired gradual change of properties along the specified direction [1]. The structures made of these materials can withstand more mechanical and thermal loads than structures made of homogeneous materials. One of the best desirable properties of these structures is preservation of its original form even when it is exposed to severe thermal load as well as mechanical loads. For example, these situations happen for turbine blades. On the other hand, the distance between the tip of the blade and engine casing is critical and it is very important to keep the clearance between the tips of rotating blades and inner surface of combustion chamber. Kapania and Raciti [2] reviewed the developments in the analysis of laminated beams and plates. This study brought together a wide range of developments and researches about the analysis of laminated plates and beams. Romano and Zingone [3] presented deformation of beams made of homogeneous materials with different rectangular cross sections. They determined relation of maximum deflection and the ratio between the minimum and the maximum height. In another study, Romano [4] presented deformation of Timoshenko beam with different forms of cross-section. Sankar [5] investigated functionally graded beams. The mechanical properties except the Poisson's ratio were assumed to vary exponentially through the thickness of the beam. Sankar and Tzeng [6] developed an analytical solution for thermoelastic response of functionally graded beams. In their study, thermal and mechanical properties except the Poisson's ratio are also variable through the thickness. Chakrabortya et al. [7] presented an exact shear deformable finite element for the analysis of FGM beams using the first-order shear deformation theory. They investigated static, free vibration and wave propagation problems in FGM beams using this method. The results showed that using first-order shear deformation theory is completely appropriate for static and dynamic analysis of FGM beams. Ching and Yen [8] presented a solution based on the meshless local Petrov–Galerkin method for transient thermoelastic deflections of FG beams. They showed that transient temperature and deformation distributions of FG beams differ from those at the steady state substantially. Also, Kadoli and et al. [9] presented stress and deformation in a special thick functional graded beam made of metal matrix composites under uniform load using higher-order shear deformation theory. They presented the results of first-order and higher-order shear deformation theory and founded that both of them yield approximately similar results. Li [10] investigated static and vibration response of FG beams under the body force. They also presented stress and deformation for a FG cantilever beam. Similar to the aforementioned researches, in this study, all material properties are assumed to vary along the thickness of the beam. Giunta et al. [11] presented linear static analysis of FGM beams using classical and axiomatic refined theories. They considered material properties exponentially varying along the one or two directions on the cross-section. The comparison of results indicated that presented higher order models are accurate and affordable in term of computational cost than finite element method. Also, they investigated thermo-mechanical response of FGM beams based on a unified formulation [12]. They validated the results obtained with finite element analysis, as in the previous article.

Rotating variable thickness FGM cantilever beam have been investigated in several literatures. Ramesh and Rao investigated the natural frequencies of vibration of a rotating pre-twisted functionally graded cantilever beam and considered the effect of coupling between chord wise and flap wise bending modes on the natural frequencies [13]. Zhang and Li investigated nonlinear vibration of rotating pre-deformed cantilever beam as a blade with thermal gradient [14]. Also, Cao et al. presented a model for rotating cantilever sandwich-plate with a pre-twisted and pre-set angle to investigate the vibrational behavior of an turbine blade with thermal barrier coating (TBC) layers [15]. Panigrahi and Pohit investigated the stiffening effect due to rotation on the nonlinear vibrational characteristics for cracked cantilever beam [16]. Functionally graded material is taken into consideration, in which the properties vary as a continuous function along the depth of the beam. Reddy [17] presented a novel model based on a modified couple stress theory for static bending, vibration and buckling analysis of homogeneous and FGM beams. One of the important advantages of this new model is that it considers the effect of FGM beam geometry on static bending, vibration and buckling. He and his colleagues [18] developed a general third-order beam theory for nonlinear analysis of TD FGM beams. They also developed nonlinear finite element model by new presented model to distinct influence of the geometric nonlinearity and microstructure-dependent constitutive relations on linear and nonlinear behavior. Kiani and Eslami [19] discussed thermal buckling and post-buckling behavior of imperfect and perfect temperature-dependent sandwich functional graded material plates. The plate is assumed to rest on the Pasternak elastic foundation and they reported post-buckling paths of two types of sandwich plates and reported the influence of their temperature dependency. Ma and Lee [20] studied the nonlinear static behavior of FGM beams while the beam is under a uniform in-plane temperature field. In another article, Nguyen et al. [21] presented a method for determination of static and dynamic behaviors of functional graded beams using the first-order shear deformation theory. The beam is considered to be only under the axial force. Niknam et al. [22] investigated non-linear bending tapered beam made of FGM under thermal and mechanical load with general boundary conditions. They plotted deflections of tapered functional graded beam subjected to various loading and boundary condition. Filippi et al. [23] presented static analysis of FGM beams by means of the 1D Carrera Unified Formulation (CUF). They showed

that features of CUF are suitable for analysis of a wide range of various structures with different boundary and loading conditions, arbitrary reinforcement distributions and shaped cross-sections and dimensions. Static response of functionally graded (FG) sandwich beams based on a quasi-3D theory is developed by Vo et al. [24]. This theory considers thickness stretching effects and shear deformation at the same time. Arefi and Zenkour [25] presented analytical solution for electro-magneto-elastic behavior of curved beam. This beam has three layers and they employed first-order shear deformation theory and the relations of motion for a beam under study. Arefi and Zenkour presented an electro-elastic analysis of a special three-layer micro-beam using combination two theories, strain gradient and higher-order sinusoidal shear deformation. They found out that the micro-length scale parameters are significantly effective on the deformation of micro-beam [26]. In another research, Ebrahimi and Jafari [27] presented an analytical method for investigating thermo-mechanical vibration of temperature-dependent functional graded beams with porosities. They developed studying for four hypothetical temperature distributions that are assumed vary along the thickness directions. A significant number of researches on the FGM beams have been dedicated to the vibration and buckling behavior of FGM beams [28-37] which are only a small number of performed studies on the behaviors for beams of these kinds. Musuva and Mares [38] presented free vibration analysis and dynamic response of a functionally graded beam under a moving point load and resting on a viscoelastic foundation. Unlike most previous similar studies, they considered the reinforcement gradation of the FGM is in the longitudinal and transverse direction based on the power law. Recently, Amlan Paul and Debabrata Das [39] presented a mathematical model to develop dynamic behavior of tapered FGM beam under thermal load considering temperature-dependent material properties. They found that temperature-dependent properties have a reasonable effect on free vibration of the beam. The literature review reveals that limited number of studies focus on the variable thickness cantilever beam made of FGM. In several literatures turbine blades modeled as cantilever beams [35, 40-43].

In this study, analysis of variable thickness cantilever beam made of FGM with temperature-dependent and temperature-independent properties is considered. Unlike previous studies, not only the material properties are variable longitudinally but also the properties are temperature-dependent and the beam geometry is also varying functionally along the beam. In this research, the model described is a simple simulation of a turbine blade working under similar loading and boundary condition.

## 2 MATERIAL PROPERTIES, GEOMETRY AND LOADING

All mechanical and thermal properties of the material are linearly variable in longitudinal direction based on the volume fraction of the constituent. Based on this assumption, properties can be described as:

$$VP(x) = V_{root} + \frac{x}{L}(V_{tip} - V_{root})$$

$$R(x, T) = R_{matrix}(x, T) + (R_{reinforcement}(x, T) - R_{matrix}(x, T)) \frac{VP(x)}{100} \quad (1)$$

where  $VP(x)$  is the volume fraction of reinforcement particles at point  $x$ ,  $V_{root}$  and  $V_{tip}$  are volume fractions of reinforcement at the root and tip of the beam, respectively. In this formula  $R$  is the property at  $x$  position and temperature  $T$ .  $R_{matrix}$  and  $R_{reinforcement}$  are the pure matrix and reinforcement property, respectively. The beam is exposed to distributed transverse forces with a specific function in terms of variable  $x$  and centrifugal force due to rotation of the beam about an axis normal to the horizontal axis.

Thermal loading is a temperature field due to thermal gradient in longitudinal direction between root and tip of the beam. Variation of the beam thickness is expressed by function  $h(x)$ . This relationship represents the profile of the beam. The geometry of the cantilever beam is shown in Fig. 1. The temperature dependency of material properties defined in Eq. (1) is taken from the literature and written as nonlinear function of temperature as [44]:

$$R_{reinforcement} \text{ or } R_{matrix} = R_0(R_{-1}T^{-1} + R_1T + R_2T^2 + R_3T^3 + 1) \quad (2)$$

Here  $T$  indicates the temperature in Kelvin and  $R_0, R_{-1}, R_1, R_2,$  and  $R_3$  are the material constants.

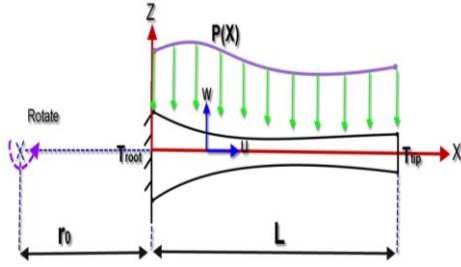


**Fig.1**  
Sketch of the cantilever beam under loading.

### 3 HEAT CONDITION PROBLEM

In steady-state conduction, the Fourier heat conduction equation in the absence of heat generation in  $x$ -direction is considered for a composite beam made of temperature-dependent material properties and is written as follows:

$$\frac{1}{x} \frac{d}{dx} (xK(x, T(x))) \frac{d}{dx} T(x) = 0 \tag{3}$$

It is supposed that the lower and upper surfaces of the cantilever beam are insulated and there is no heat loss. If the thermal conductivity is assumed to be TID, then Eq. (3) becomes a second-order ordinary differential equation the solution of which gives the temperature distribution for this case. However, in the case of TD the coefficients are variable in longitudinal direction. Because of longitudinal-dependent of coefficients, a semi analytical method [41] is employed to solve the differential equation. In this method, the FGM beam is divided into a large number of divisions longitudinally. The schematic of the beam and sample of divisions is depicted in Fig. 2.

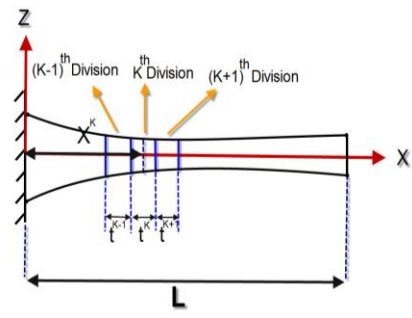


**Fig.2**  
Dividing  $x$ -direction of cantilever FGM beam.

The coefficients of second-order ordinary differential equation (SODE) are calculated at  $x(k)$ , midpoint of  $K^{th}$  division and the differential equation and specified coefficients are only valid in  $K^{th}$  division and is rewritten as:

$$\left( \frac{d^2}{dx^2} + S^{(k)} \frac{d}{dx} \right) T = 0 \tag{4}$$

where

$$S^{(k)} = \frac{1}{x^{(k)}} + \frac{1}{K_T(x^{(k)})} \frac{dK_T(x)}{dx} \Bigg|_{x=x^{(k)}} \quad k = 1, 2, \dots, m \tag{5}$$

The SODE with variable coefficients is turned into SODE with constant coefficients for each section. The solution of mentioned SODEs is exactly expressed as:

$$T(x^{(k)}) = \bar{R}_1^{(k)} + \bar{R}_2^{(k)} \exp(-x^{(k)} S^{(k)}) \tag{6}$$

where  $\bar{R}_1^{(k)}$  and  $\bar{R}_2^{(k)}$  are unknowns constants for  $K^{th}$  subdomain. These constants can be determined using the continuity condition of temperature and the continuity condition of thermal conduction at the interfaces of the adjacent sub-domains. These continuity conditions at the interfaces are:

$$\begin{aligned} T(x) \Big|_{x=x^k+\frac{t^k}{2}} &= T(x) \Big|_{x=x^{k+1}-\frac{t^{k+1}}{2}} \\ \frac{dT(x)}{dx} \Big|_{x=x^k+\frac{t^k}{2}} &= \frac{dT(x)}{dx} \Big|_{x=x^{k+1}-\frac{t^{k+1}}{2}} \end{aligned} \quad (7)$$

The global boundary conditions on the root and tip surfaces of the FGM beam must also be satisfied. These are:

$$\begin{aligned} T(x_{root}) &= T_{root} \\ T(x_{tip}) &= T_{tip} \end{aligned} \quad (8)$$

Eq. (7) together with Eq. (8) constructs a set of linear algebraic equations with regard to  $\bar{R}_1^{(k)}$  and  $\bar{R}_2^{(k)}$  coefficients. Solving these equations with respect to  $\bar{R}_1^{(k)}$  and  $\bar{R}_2^{(k)}$ , temperature distribution  $T(x)$  can be achieved in each division. For the cases of TD thermal conductivity, Eq. (4) is implicit with the function  $T(x)$  and therefore necessitates an iterative algorithm obtain the exact temperature distribution. To solve differential Eq. (4), a successive solution method is employed [46]. Step-by-step algorithm is extensively presented as follows:

- 1- Particular estimated values of temperature are considered at each sub-domain.
- 2- With the assumed distribution for temperature,  $K(x)$  is computed for the constituents using Eq. (2) and Eq. (3).
- 3- Using these values of  $K(x)$  from step 2 at all division points, a new temperature distribution is obtained which is compared with the previous estimated values at all division points for the convergence of the procedure. If convergence is achieved for all division points, then iteration will be stopped. Otherwise, these new achieved values of temperature distribution will be considered as initial distribution for temperature and the algorithm will be repeated until convergence is obtained.

#### 4 GOVERNING EQUATIONS AND ANALYSIS METHOD

In this section, by the FSDT, an elastic solution is presented. The displacements in the  $X$  and  $Z$  directions are in accordance with the theory of elasticity as:

$$\begin{cases} u(x, z) = u_0 + z\psi(x) \\ w(x, z) = w_0 \end{cases} \quad (9)$$

where here,  $u_0$  shows the longitudinal displacement of the neutral axis,  $w_0$  represents the transverse displacement of the neutral axis in the thickness direction and  $\psi(x)$  is rotation component. Using the linear strain–displacement relations and also considering thermal strain, longitudinal and shear strain components are written as:

$$\begin{aligned} \varepsilon_{xx} &= \frac{\partial u}{\partial x} = \frac{\partial u_0}{\partial x} + z \frac{\partial \psi(x)}{\partial x} + \alpha T(x) \\ \gamma_{xz} &= \frac{\partial u}{\partial z} + \frac{\partial w}{\partial x} = \psi(x) + \frac{\partial w_0}{\partial x} + \dots \end{aligned} \quad (10)$$

Generalized Hooke's law by considering the thermal strains is written as:

$$\begin{aligned}\sigma_{xx} &= E\varepsilon_{xx} = E \left[ \frac{\partial u_0}{\partial x} + z \frac{\partial \psi(x)}{\partial x} + \alpha T(x) \right] \\ \tau_{xz} &= G\gamma_{xz} = G \left[ \psi(x) + \frac{\partial w_0}{\partial x} \right]\end{aligned}\quad (11)$$

The variation of the strain energy in accordance with the principle of virtual work is:

$$\begin{aligned}\delta U &= \int \int_{AZ} (\sigma_{xx} \delta \varepsilon_{xx} + \tau_{xz} \delta \gamma_{xz}) dz dA = \\ &= \int \int_{AZ} \left( \sigma_{xx} \left( \frac{\partial \delta u_0}{\partial x} + z \frac{\partial \delta \psi(x)}{\partial x} + \delta \alpha T(x) \right) + \tau_{xz} \left( \delta \psi(x) + \frac{\partial \delta w_0}{\partial x} \right) \right) dz dA = \\ &= \int_A \left( N_{xx} \frac{\partial \delta u_0}{\partial x} + M_{xx} \frac{\partial \delta \psi(x)}{\partial x} + N_{xz} \delta \psi(x) + N_{xz} \frac{\partial \delta w_0}{\partial x} \right) dA\end{aligned}\quad (12)$$

The resultant force and moment per unit length due to stresses are equal to:

$$\begin{aligned}N_{xx} &= \int \sigma_{xx} dz = \left[ \int E(x) dz \right] \frac{\partial u_0}{\partial x} + \left[ \int z E(x) dz \right] \frac{\partial \psi}{\partial x} + \int E(x) \alpha(x) T(x) dz \\ N_{xz} &= \int \sigma_{xz} dz = \left[ \int G(x) dz \right] \left[ \psi(x) + \frac{\partial w_0}{\partial x} \right] \\ M_{xx} &= \int z \sigma_{xx} dz = \left[ \int z E(x) dz \right] \frac{\partial u_0}{\partial x} + \left[ \int z^2 E(x) dz \right] \frac{\partial \psi}{\partial x} + \int E(x) \alpha(x) T(x) z dz\end{aligned}\quad (13)$$

The external work is represented by:

$$W = - \int_z (F_1(x)u + F_2(x)\psi + F_3(x)w) dx \quad (14)$$

where

$$F(x) = \begin{bmatrix} F_1(x) \\ F_2(x) \\ F_3(x) \end{bmatrix} = \begin{bmatrix} \omega^2 \rho(x) h(x) [r_0 + x] \\ 0 \\ -P(x) \end{bmatrix} \quad (15)$$

According to Eq. (8), variation of external work is expressed as:

$$\delta W = - \int_z (F_1(x) \delta u + F_2(x) \delta \psi + F_3(x) \delta w) dx \quad (16)$$

Based on the principle of virtual work, the strain energy variations are equal to the variation of external work, namely:

$$\delta U = \delta W \quad (17)$$

The following relationships are obtained according to (12) and the use of the variation calculus.

$$\begin{aligned}\frac{\partial N_{xx}}{\partial x} + A_5(x) T(x) &= F_1(x) \\ -\frac{\partial M_{xx}}{\partial x} + N_{xz} &= 0 \\ \frac{\partial N_{xz}}{\partial x} + A_6(x) T(x) &= F_3(x)\end{aligned}\quad (18)$$

By substituting from relation (13) into Eq. (18) the following constitutive differential equations of the problem are obtained.

$$\begin{aligned} A_1(x)u_{,xx} + A_2(x)\psi_{,xx} + A_5(x)T(x) &= F_1(x) \\ -A_2(x)u_{,xx}(x) - A_4(x)\psi_{,xx}(x) + A_3(x)\psi(x) + A_3(x)w_{,x}(x) &= 0 \\ A_3(x)\psi_{,x}(x) + A_3(x)w_{,xx}(x) + A_6(x)T(x) &= F_3(x) \end{aligned} \quad (19)$$

where  $A_i(x)$  ( $i=1,2,3,4,5,6$ ) is given in the Appendix A. To solve these differential equations with variable coefficients a semi analytical division method has been used [45].

A large number of divisions in longitudinal direction are considered. For the center point of each division, the Eqs. (19) are solved and, using the local boundary conditions introduced in relations (20), and global boundary condition (21), a set of algebraic equations containing constant coefficients of each division are obtained. Solving these equations constants are obtained, then displacements, stresses and strains are achieved.

The local boundary conditions that are due to the continuity condition are:

$$\begin{aligned} u\left(x^k + \frac{t^k}{2}\right) &= u\left(x^{k+1} - \frac{t^{k+1}}{2}\right) \\ \psi\left(x^k + \frac{t^k}{2}\right) &= \psi\left(x^{k+1} - \frac{t^{k+1}}{2}\right) \\ w\left(x^k + \frac{t^k}{2}\right) &= w\left(x^{k+1} - \frac{t^{k+1}}{2}\right) \\ u_{,x}\left(x^k + \frac{t^k}{2}\right) &= u_{,x}\left(x^{k+1} - \frac{t^{k+1}}{2}\right) \\ \psi_{,x}\left(x^k + \frac{t^k}{2}\right) &= \psi_{,x}\left(x^{k+1} - \frac{t^{k+1}}{2}\right) \\ w_{,x}\left(x^k + \frac{t^k}{2}\right) &= w_{,x}\left(x^{k+1} - \frac{t^{k+1}}{2}\right) \end{aligned} \quad (20)$$

and the root and tip boundary conditions of the cantilever FGM beam are:

$$\begin{aligned} B.C. : \begin{cases} u = 0 \\ \psi = 0 \\ w = 0 \end{cases} & \quad x = 0 \\ B.C. : \begin{cases} N_{xz} = \int \tau(x, z) dA = 0 \\ M_{xx} = \int z \sigma_{xx} dA = 0 \\ N_{xx} = \int \sigma_{xx} dA = 0 \end{cases} & \quad x = L \end{aligned} \quad (21)$$

In this method, for  $K^{th}$  division, Eqs. (19) is rewritten as follows:

$$\begin{aligned} A_1(x^k)u_{,xx} + A_2(x^k)\psi_{,xx} + A_5(x^k)T(x^k) &= F_1(x^k) \\ -A_2(x^k)u_{,xx}(x^k) - A_4(x^k)\psi_{,xx}(x^k) + A_3(x^k)\psi(x^k) + A_3(x^k)w_{,x}(x^k) &= 0 \\ A_3(x^k)\psi_{,x}(x^k) + A_3(x^k)w_{,xx}(x^k) + A_6(x^k)T(x^k) &= F_3(x^k) \end{aligned} \quad (22)$$

where the constants  $A_i(x^k)$  ( $i=1,2,3,4,5,6$ ) are given in the Appendix B.

## 5 NUMERICAL RESULTS

An analysis is performed for a cantilever FGM beam whose non-homogeneity is due to variable property in longitudinal direction, using the method described in the previous section. Upper and lower surfaces profiles are mathematically represented by the following relations (23) and (24). In these equations  $x$  is in millimeter.

$$14e^{-0.01x} + \frac{x}{30} \quad (23)$$

$$-14e^{-0.01x} - \frac{x}{30} \quad (24)$$

with the above mentioned profiles thickness as a function of  $x$  is represented by Eq. (25).

$$h(x) = 28e^{-0.01x} - \frac{x}{15} \quad (25)$$

To find the thermoelastic response of a FGM cantilever beam, studies have been carried out based on  $ZrO_2 / Ti6Al4V$  constituent. However, the mentioned method in this paper is as well applicable for every type of functional graded materials. The TD properties corresponding to  $ZrO_2$  and  $Ti6Al4V$  are given in Table 1. In this composite, Poisson's ratio is constantly supposed and  $\nu = 0.29$ . Also, it is assumed that  $L = 200 \text{ mm}$ ,  $r_0 = 300 \text{ mm}$ ,  $T_{root} = 300 \text{ K}$ ,  $T_{tip} = 700 \text{ K}$ ,  $\rho_{ZrO_2} = 5680 \text{ kg} / \text{m}^3$ ,  $\rho_{Ti6Al4V} = 4429 \text{ kg} / \text{m}^3$ ,  $\omega = 3000 \text{ rpm}$ .

**Table1**

Temperature-dependent coefficients for  $ZrO_2$  and  $Ti6Al4V$  [47].

Metal & Reinforcement	$R_0$	$R_{-1}$	$R_1$	$R_2$	$R_3$
$ZrO_2$					
$E(Pa)$	244.27e+9	0	-1.371e-3	1.214e-6	-3.681e-10
$\alpha(K^{-1})$	12.766e-6	0	-1.491e-3	1.006e-5	-6.778e-11
$K(w/m^0K)$	1.7000	0	1.27e-4	6.648e-8	0
$Ti6Al4V$					
$E(Pa)$	122.56e+9	0	-4.586e-4	0	0
$\alpha(K^{-1})$	7.5788e-6	0	6.638e-4	-0.3147e-6	0
$K(w/mk)$	1.0000	0	1.704e-2	0	0

The distributed force  $P(x)$  is variable from the root to the tip of the beam linearly and is represented by relation (26).

$$P(x) = 0.03x + 0.05 \quad (26)$$

For three different cases of reinforcement volume content distributions  $A : V_{root} = 0, V_{tip} = 30$ ,  $B : V_{root} = 30, V_{tip} = 0$  and  $C : V_{root} = 15, V_{tip} = 15$ , the temperature distribution, longitudinal and transverse displacements, longitudinal shear and effective stresses are calculated by the present method. Schematic of the three different cases of reinforcement distributions of the beam are illustrated in Fig 3.

Figs. 4-9 are devoted to temperature distribution, longitudinal displacement distribution, transverse displacement distribution, transverse stress distribution, shear stress distribution and effective stress distribution of all three cases considering TID and TD properties non-dimensionally.

To demonstrate the precision and validity of the current study, using Abaqus software, temperature distribution, displacements distribution and stresses distribution are calculated for the case B-TD and compared with the same case obtained from the proposed method. The A-TD and B-TD are general cases because in these cases, material properties are temperature-dependent and functionally. Note that in these figures, dash line and solid line correspond to TD and TID properties respectively.

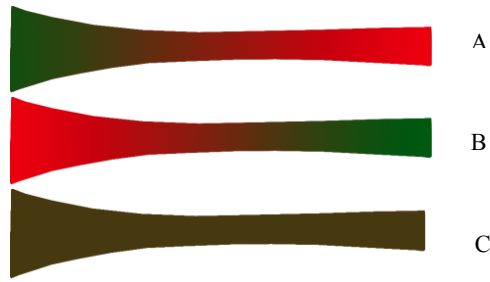


**Fig.3**  
Schematic of the three different reinforcement distributions of the beam.

**6 DISCUSSION**

Fig. 4 shows that the boundary condition for temperature distribution is satisfied at the root and the tip of the beam, however the temperature distribution for the TD property case is higher than TID property. It is interesting that the temperature of the corresponding point in TID in case *A* is higher than case *C* and in the case *C* is higher than *B* and this trend is the same for TD properties, i.e. the temperature in case *A* is higher than *C*, and in case *C* is higher than *B*. At lower temperatures near the root and for the TD cases, according to Eq. (1) and (2) and Table 1., the heat conduction coefficient is lower which is associated with higher temperature gradient due to the same heat flux throughout the beam. On the other hand, at the higher temperature of the tip region, lower temperature gradient is expected as is evident from the Fig. 4. A convex curve for temperature distribution in these cases is therefore justified.

In TID cases the temperature distribution dependent on volume percent distribution of reinforcement. For the *A*-TID case the heat conduction coefficient is lower at the root and higher at the tip which is associated with higher gradient at the root and lower at the tip yielding to a low convex shape for temperature distribution. The concave curve of temperature distribution for the case *B*-TID is due to higher content of reinforcement at the root and lower values at the tip.

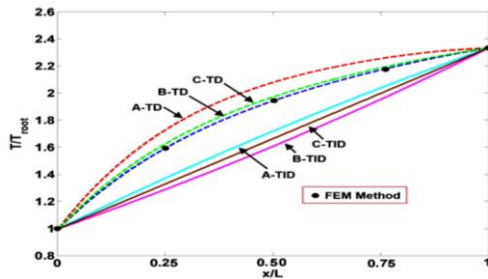


**Fig.4**  
Temperature distribution of composite cantilever beam.

Longitudinal displacement is depicted in Fig. 5. Generally, the longitudinal displacement is positive which is due to centrifugal body force. It is zero at the root and is maximum at the tip for all cases and material properties which is expected from the boundary condition. It is obvious that the longitudinal displacements for the TID properties are lower than TD. Since for the TD cases, values of elastic and shear modulus *E* and *G* are lower according to Eq. (1) and Eq. (2) and Table 1., therefore, higher elongation is justified for TD cases. For the case *B* the reinforcement content at the thicker root region is higher than the tip therefore the beam mass will be higher in this case and a higher centrifugal force is expected.

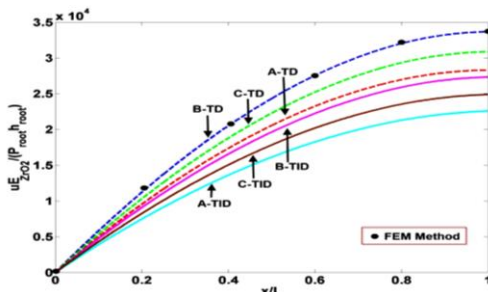


**Fig.5**  
Longitudinal displacement distribution of composite cantilever beam.

Transverse displacement of the composite cantilever beam is shown in Fig. 6. The transverse displacement is negative because of the downward distributed force over the beam. It is zero at the root and its maximum absolute value is located at the tip for all cases and material properties as expected from the boundary condition. All cases of reinforcement content and material temperature dependency and independency have not significant effect on transverse displacement almost on the first half of the beam. Since elastic and shear modulus of the TD cases are lower than TID cases, their absolute values of transverse displacement are higher.

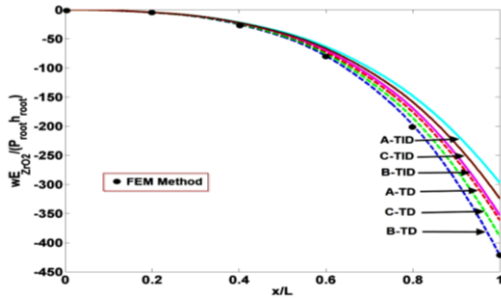


**Fig.6**  
Transverse displacement distribution of composite cantilever beam.

Fig. 7 shows the longitudinal tensile stress which is maximum at the root and is zero at the tip which satisfies the free boundary condition at the tip and maximum centrifugal force at the root. The longitudinal stress in TD properties is basically higher than TID properties. In addition, for TD or TID properties, the longitudinal stress for the case A is lower than C and for the case C is lower than B. The same trend is observed in Figs. 8 and 9.

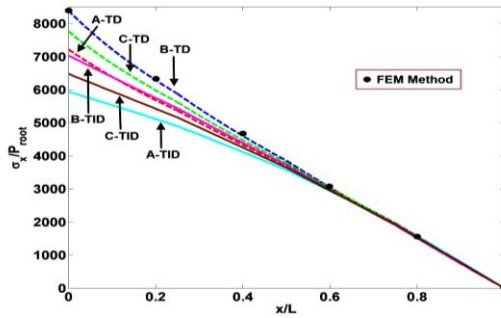


**Fig.7**  
Longitudinal stress distribution of composite cantilever beam.

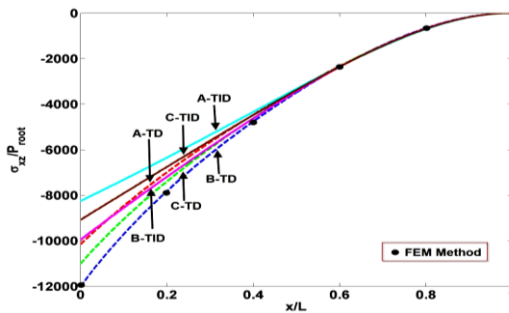


**Fig.8**  
Transverse stress distribution of composite cantilever beam.

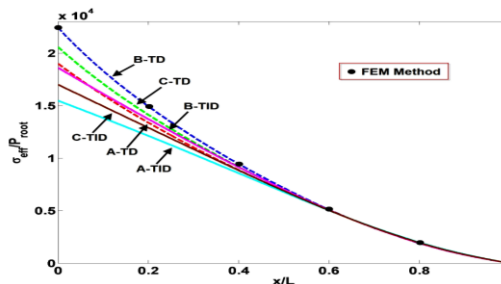


**Fig.9**  
Effective stress distribution of composite cantilever beam.

Material temperature dependency/independency and reinforcement distribution have not considerable effect on longitudinal stress almost on the second half of the beam. It demonstrates that by considering the FGM materials with temperature dependent properties, the stress and displacements will both increase. Moreover, the volume content distribution of the reinforcement has considerable effects on stress and displacements. For example, for this specific case, as expected, the maximum effective stress happens at the root of the beam and in case TD with distribution  $B$  (solid line  $B$ -TD), the value of maximum effective stress is 1.44 times more than in case TID with distribution  $A$  (solid line  $A$ -TID). Also in case TD with distribution  $B$  (solid line  $B$ -TD), the maximum longitudinal displacement is 1.5 times higher than that in case TID with distribution  $A$  (dashed line  $A$ -TID).

It is seen from Figs. 4-9 that there is a good agreement between the method presented in this study and the finite element method.

## 7 CONCLUSIONS

In this paper, a semi-analytic method is employed for analysis of a variable thickness cantilever beam (VTCB) subjected to thermomechanical loading. The beam is made of a metal based composite reinforced by a ceramic, the volume content of which is linearly distributed in longitudinal direction so that the material property is variable based on the constituent volume fraction. Two different cases of temperature-dependent and temperature-independent properties are studied. It is noteworthy to mention that except the Poisson coefficient, rest of the thermal and mechanical properties are assumed to be variable along the beam. By successive relaxation method (SR), the temperature distribution along the beam is obtained. In fact, this beam is a simplified model of the turbine's blade. The distributed force represents the aerodynamic force on the blade. Using first-order shear deformation theory, linear strain–displacement relations and Generalized Hooke's law, a system of the second order differential equations (SODE) is obtained. Because of variable coefficients due to variable properties, a division method is applied to solve the differential equations. The coefficients then become constant for each division. An analysis is done for a beam made of  $ZrO_2/Ti6Al4V$  composite and the results for a most general case are validated by the finite element method. The results indicated that consideration of temperature dependency for the functionally graded material has a significant influence on the temperature, displacements and stresses. Moreover, the results are presented for three different cases of reinforcement distribution the influence of which on temperature, displacements and stresses are also considerable.

## ACKNOWLEDGEMENT

This work was supported by the University of Kashan under Grant number: 468797.

## APPENDIX A

$$A_i(x) (i = 1, 2, 3, 4, 5, 6)$$

$$A_1(x) = \int_{-0.5h(x)}^{0.5h(x)} E(x) dz \quad A_2(x) = \int_{-0.5h(x)}^{0.5h(x)} zE(x) dz \quad A_3(x) = \int_{-0.5h(x)}^{0.5h(x)} G(x) dx$$

$$A_4(x) = \int_{-0.5h(x)}^{0.5h(x)} z^2 E(x) dz \quad A_5(x) = \int_{-0.5h(x)}^{0.5h(x)} E(x) \alpha(x) dz \quad A_6(x) = \int_{-0.5h(x)}^{0.5h(x)} E(x) \alpha(x) z dz$$

## APPENDIX B

$$A_i(x^k) (i = 1, 2, 3, 4, 5, 6)$$

$$A_1(x^k) = \int_{-0.5h(x^k)}^{0.5h(x^k)} E(x^k) dz \quad A_2(x^k) = \int_{-0.5h(x^k)}^{0.5h(x^k)} zE(x^k) dz \quad A_3(x^k) = \int_{-0.5h(x^k)}^{0.5h(x^k)} G(x^k) dx$$

$$A_4(x^k) = \int_{-0.5h(x^k)}^{0.5h(x^k)} z^2 E(x^k) dz \quad A_5(x^k) = \int_{-0.5h(x^k)}^{0.5h(x^k)} E(x^k) \alpha(x^k) T(x^k) dz$$

## REFERENCES

- [1] Yamanouti M., Koizumi M., Shiota I., 1990, Functionally gradient materials forum, *Proceedings of the First International Symposium on Functionally Gradient Materials*, Sendai, Japan.
- [2] Kapania R.K., Raciti S., 1989, Recent advances in analysis of laminated beams and plates, Part I - Sheareffects and buckling, *AIAA Journal* **27**(7): 923-935.
- [3] Romano F., Zingone G., 1992, Deflections of beams with varying rectangular cross section, *Journal of Engineering Mechanics* **118**(10): 2128-2134.
- [4] Romano F., 1996, Deflections of Timoshenko beam with varying cross-section, *International Journal of Mechanical Sciences* **38**(8): 1017-1035.
- [5] Sankar B.V., 2001, An elasticity solution for functionally graded beams, *Composites Science and Technology* **61**(5): 689-696.
- [6] Sankar B.V., Tzeng J.T., 2002, Thermal stresses in functionally graded beams, *AIAA Journal* **40**(6): 1228-1232.
- [7] Chakraborty A., Gopalakrishnan S., Reddy J.N., 2003, A new beam finite element for the analysis of functionally graded materials, *International Journal of Mechanical Sciences* **45**(3): 519-539.
- [8] Ching H.K., Yen S.C., 2006, Transient thermoelastic deformations of 2-D functionally graded beams under nonuniformly convective heat supply, *Composite Structures* **73**(4): 381-393.
- [9] Kadoli R., Akhtar K., Ganesan N., 2008, Static analysis of functionally graded beams using higher order shear deformation theory, *Applied Mathematical Modelling* **32**(12): 2509-2525.
- [10] Li X.F., 2008, A unified approach for analyzing static and dynamic behaviors of functionally graded Timoshenko and Euler-Bernoulli beams, *Journal of Sound and Vibration* **318**(4): 1210-1229.
- [11] Giunta G., Belouettar S., Carrera E., 2010, Analysis of FGM beams by means of classical and advanced theories, *Mechanics of Advanced Materials and Structures* **17**(8): 622-635.
- [12] Giunta G., Crisafulli D., Belouettar S., Carrera E., 2013, A thermo-mechanical analysis of functionally graded beams via hierarchical modelling, *Composite Structures* **95**: 676-690.
- [13] Ramesh M.N.V., Mohan Rao N., 2013, Free vibration analysis of pre-twisted rotating FGM beams, *International Journal of Mechanics and Materials in Design* **9**(4): 367-383.
- [14] Zhang B., Li Y., 2016, Nonlinear vibration of rotating pre-deformed blade with thermal gradient, *Nonlinear Dynamics* **86**(1): 459-478.
- [15] Cao D., Liu B., Yao B., Zhang W., 2017, Free vibration analysis of a pre-twisted sandwich blade with thermal barrier coatings layers, *Science China Technological Sciences* **60**(11): 1747-1761.
- [16] Panigrahi B., Pohit G., 2018, Effect of cracks on nonlinear flexural vibration of rotating Timoshenko functionally graded material beam having large amplitude motion, *Proceedings of the Institution of Mechanical Engineers, Part C: Journal of Mechanical Engineering Science* **232**(6): 930-940.
- [17] Reddy J.N., 2011, Microstructure-dependent couple stress theories of functionally graded beams, *Journal of the Mechanics and Physics of Solids* **59**(11): 2382-2399.
- [18] Arbind A., Reddy J.N., Srinivasa A.R., 2014, Modified couple stress-based third-order theory for nonlinear analysis of functionally graded beams, *Latin American Journal of Solids and Structures* **11**: 459-487.
- [19] Kiani Y., Eslami M.R., 2012, Thermal buckling and post-buckling response of imperfect temperature-dependent sandwich FGM plates resting on elastic foundation, *Archive of Applied Mechanics* **82**(7): 891-905.
- [20] Ma L.S., Lee D.W., 2012, Exact solutions for nonlinear static responses of a shear deformable FGM beam under an in-plane thermal loading, *European Journal of Mechanics - A/Solids* **31**(1): 13-20.
- [21] Nguyen T.-K., Vo T.P., Thai H.-T., 2013, Static and free vibration of axially loaded functionally graded beams based on the first-order shear deformation theory, *Composites Part B: Engineering* **55**: 147-157.
- [22] Niknam H., Fallah A., Aghdam M.M., 2014, Nonlinear bending of functionally graded tapered beams subjected to thermal and mechanical loading, *International Journal of Non-Linear Mechanics* **65**: 141-147.
- [23] Filippi M., Carrera E., Zenkour A.M., 2015, Static analyses of FGM beams by various theories and finite elements, *Composites Part B: Engineering* **72**: 1-9.
- [24] Vo T.P., Thai H.-T., Nguyen T.-K., Inam F., Lee J., 2015, Static behaviour of functionally graded sandwich beams using a quasi-3D theory, *Composites Part B: Engineering* **68**: 59-74.
- [25] Arefi M., Zenkour A.M., 2017, Electro-magneto-elastic analysis of a three-layer curved beam, *Smart Structures and Systems* **19**(6): 695-703.
- [26] Arefi M., Zenkour A.M., 2017, Size-dependent electro-elastic analysis of a sandwich microbeam based on higher-order sinusoidal shear deformation theory and strain gradient theory, *Journal of Intelligent Material Systems and Structures* **29**(7): 1394-1406.

- [27] Ebrahimi F., Jafari A., 2018, A four-variable refined shear-deformation beam theory for thermo-mechanical vibration analysis of temperature-dependent FGM beams with porosities, *Mechanics of Advanced Materials and Structures* **25**(3): 212-224.
- [28] Oh S.-Y., Librescu L., Song O., 2003, Vibration of turbomachinery rotating blades made-up of functionally graded materials and operating in a high temperature field, *Acta Mechanica* **166**(1): 69-87.
- [29] Karami Khorramabadi M., 2009, Free vibration of functionally graded beams with piezoelectric layers subjected to axial load, *Journal of Solid Mechanics* **1**(1): 22-28.
- [30] Shahba A., Attarnejad R., Marvi M.T., Hajilar S., 2011, Free vibration and stability analysis of axially functionally graded tapered Timoshenko beams with classical and non-classical boundary conditions, *Composites Part B: Engineering* **42**(4): 801-808.
- [31] Yas M.H., Kamarian S., Jam J.E., Pourasghar A., 2011, Optimization of functionally graded beams resting on elastic foundations, *Journal of Solid Mechanics* **3**(4): 365-378.
- [32] Huang Y., Yang L.-E., Luo Q.-Z., 2013, Free vibration of axially functionally graded Timoshenko beams with non-uniform cross-section, *Composites Part B: Engineering* **45**(1): 1493-1498.
- [33] Mashat D.S., Carrera E., Zenkour A.M., Al Khateeb S.A., Filippi M., 2014, Free vibration of FGM layered beams by various theories and finite elements, *Composites Part B: Engineering* **59**: 269-278.
- [34] Jafari-Talookolaei R.A., 2015, Analytical solution for the free vibration characteristics of the rotating composite beams with a delamination, *Aerospace Science and Technology* **45**: 346-358.
- [35] Oh Y., Yoo H.H., 2016, Vibration analysis of rotating pretwisted tapered blades made of functionally graded materials, *International Journal of Mechanical Sciences* **119**: 68-79.
- [36] Carrera E., Pagani A., Banerjee J.R., 2016, Linearized buckling analysis of isotropic and composite beam-columns by Carrera Unified Formulation and dynamic stiffness method, *Mechanics of Advanced Materials and Structures* **23**(9): 1092-1103.
- [37] Rafiee M., Nitzsche F., Labrosse M., 2017, Dynamics, vibration and control of rotating composite beams and blades: A critical review, *Thin-Walled Structures* **119**: 795-819.
- [38] Musuva M., Mares C., 2015, The wavelet finite element method in the dynamic analysis of a functionally graded beam resting on a viscoelastic foundation subjected to a moving load, *European Journal of Computational Mechanics* **24**(5): 171-209.
- [39] Paul A., Das D., 2018, Free vibration behavior of tapered functionally graded material beam in thermal environment considering geometric non-linearity, shear deformability and temperature-dependent thermal conductivity, *Proceedings of the Institution of Mechanical Engineers, Part L: Journal of Materials: Design and Applications*.
- [40] Shankar K.A., Pandey M., 2016, Nonlinear dynamic analysis of cracked cantilever beam using reduced order model, *Procedia Engineering* **144**: 1459-1468.
- [41] Babu K.R.P., Kumar B.R., Rao K.M., 2016, Modal testing and finite element analysis of crack effects on turbine blades, *Journal of Solid Mechanics* **8**(3): 614-624.
- [42] Beglinger V., Bolleter U., Locher W.E., 1976, Effects of shear deformation, rotary inertia, and elasticity of the support on the resonance frequencies of short cantilever beams, *Journal of Engineering for Power* **98**(1): 79-87.
- [43] Reinhardt A.K., Kadambi J.R., Quinn R.D., 1995, Laser vibrometry measurements of rotating blade vibrations, *Journal of Engineering for Gas Turbines and Power* **117**(3): 484-488.
- [44] Touloukian Y.S., 1967, *Thermophysical Properties of High Temperature Solid Materials: Elements*, A.F.M. Laboratory, Macmillan.
- [45] Kordkheili S.A.H., Naghdabadi R., 2007, Thermoelastic analysis of a functionally graded rotating disk, *Composite Structures* **79**(4): 508-516.
- [46] Cook R.D., 2001, *Concepts and Applications of Finite Element Analysis*, Wiley.
- [47] Shen H.-S., Li S.-R., 2008, Postbuckling of sandwich plates with FGM face sheets and temperature-dependent properties, *Composites Part B: Engineering* **39**(2): 332-344.